CHEMISTRY OF MATERIALS

ARTICLE

pubs.acs.org/cm

Incorporating Benzotriazole Moiety to Construct D−A−π−A Organic Sensitizers for Solar Cells: Significant Enhancement of Open-Circuit Photovoltage with Long Alkyl Group

Yan Cui,[†,‡] Yongzhen Wu,[†,§] Xuefeng Lu,[‡] Xi Zhang,[‡] Gang Zhou,[*,‡] Fohn B. Miapeh,[§] Weihong Zhu,[*,§] and Zhong-Sheng Wang[*,‡]

[‡]Department of Macromolecular Science, Department of Chemistry and Laboratory of Advanced Materials, Fudan University, Shanghai 200438, P. R. China

[§]Shanghai Key Laboratory of Functional Materials Chemistry, Key Laboratory for Advanced Materials and Institute of Fine Chemicals, East China University of Science and Technology, Shanghai 200237, P. R. China

Supporting Information

ABSTRACT: Two novel benzotriazole-containing organic dyes based on D−A−π−A configuration, **WS-5** with octyl group and **WS-8** with methyl group, have been designed and synthesized for use in dye-sensitized solar cells (DSSCs). Compared with the traditional D−π−A sensitizers, the benzotriazole unit as an additional acceptor has several merits: (i) essentially facilitating the electron transfer from the donor to the acceptor/anchor; (ii) conveniently tailoring the solar cell performance with a facile structural modification on 2-position in the benzotriazole unit; and (iii) the nitrogen-containing heterocyclic group of benzotriazole being expected to improve the open-circuit photovoltage. The analysis of controlled intensity modulated photovoltage spectroscopy reveals that the replacement of methyl with octyl group enhances electron lifetime by 4-fold and retards charge recombination rate constant by 4-fold. The two dye-loaded TiO_2 films possess almost the same conduction band position under the same condition, as revealed by the charge densities at open-circuit against open-circuit photovoltage. Therefore, the significant enhancement of open-circuit photovoltage from methyl to octyl group is attributed to the suppressed charge recombination. Under simulated AM1.5G solar light (100 mW cm^{-2}), the DSSC based on **WS-5** produces a short-circuit photocurrent of 13.18 mA cm^{-2}, an open-circuit photovoltage of 0.78 V, a fill factor of 0.78, corresponding to a power conversion efficiency of 8.02%.

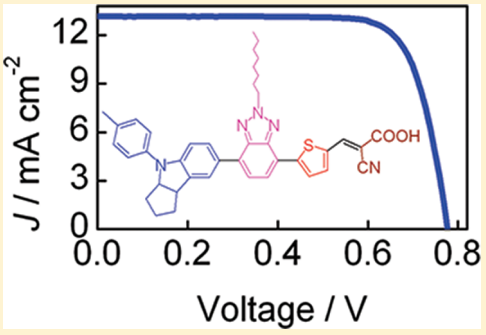

KEYWORDS: dye sensitizers, solar cells, benzotriazole, open-circuit photovoltage, charge recombination

INTRODUCTION

Since the discovery by Grätzel and co-workers in 1991,[1] dye-sensitized solar cells (DSSCs) have attracted extensive attention in the last two decades because of the efficient conversion of solar energy to electricity at a low cost.[2] Up to date, such cells employing ruthenium (Ru) polypyridyl complexes as sensitizers have achieved power conversion efficiencies of 11−12% under standard global air mass 1.5 (AM1.5G).[3] However, in view of cost and limited availability of Ru complexes, alternative metal-free organic dyes,[4] commonly constructed with donor−π-bridge−acceptor (D−π−A) configuration, are strongly desirable because of the following features:[4,5] (i) larger absorption coefficients (attributed to an intramolecular π−π* transition) than metal complex photosensitizers (attributed to metal-to-ligand charge transfer), leading to more efficient light-harvesting; (ii) the feasibilities and varieties in molecular designs for easy control of their optoelectronic properties; and (iii) no concern on the limited resource of noble metals, such as ruthenium. To date, DSSCs based on metal-free organic sensitizers have been receiving much attention, especially in cost-effective facile preparation processes. However, the power conversion efficiencies of organic sensitizer-based cells are generally lower than those based on Ru complex sensitizers. The major reason is the relatively low open-circuit photovoltage (V_{oc}) for metal-free DSSCs, possibly arising from shorter electron lifetime in comparison to the DSSCs based on the Ru dyes.[5c] Recently, Tian et al. have discussed the effects of charge recombination and electron injection efficiency on V_{oc}, formulating basic guidelines and strategies for improving V_{oc} and the overall performance of DSSCs.[4c]

Among metal-free organic sensitizers, the D−π−A structure is the most common character of these organic dyes,[4] which has been well-demonstrated to extend the absorption spectra, adjust the HOMO and LUMO levels, and realize the intramolecular charge separation. Recently, D−A−π−A configuration with benzothiadiazole,[6a,b] quinoxaline,[6c] and cyano[6d] groups as acceptors has been designed and attracted more attention because

Received: August 1, 2011
Revised: August 26, 2011
Published: September 13, 2011

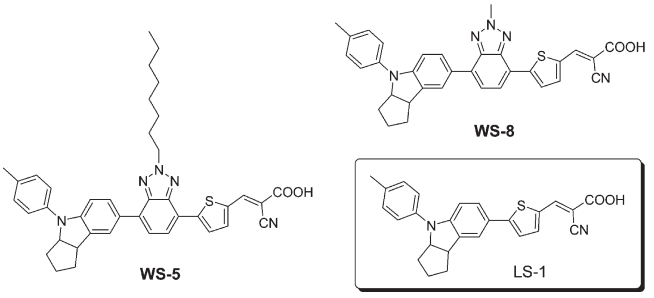

Figure 1. Chemical structures of D−A−π−A sensitizers **WS-5** and **WS-8** containing low band gap and strong electron-withdrawing unit of benzotriazole as additional acceptor, and reference dye LS-1.

the additional acceptor chromophore is expected to facilitate the electron transfer from the donor to the acceptor/anchor (i.e., cyanoacetic unit). To distinguish our designed structure from the typical D−π−A configuration and emphasize the role of benzotriazole unit, we herein refer our dyes to the D−A−π−A structured dyes. The presence of two acceptors in the nomenclature does not mean two discrete, spatially separated LUMO orbitals present in the molecule. In fact, the LUMO orbital is delocalized over the A−π−A units, which are therefore a single acceptor unit.

Benzotriazole, a very cheap and commercially available material, has been employed to construct low band gap copolymers for bulk-heterojunction solar cells because of its unique electron-accepting properties.[7] However, the utilization of benzotriazole unit in molecular sensitizers for DSSCs has not been reported so far to the best of our knowledge. Herein, the benzotriazole unit was incorporated into indoline based organic dyes to further develop novel D−A−π−A configuration sensitizers (**WS-5** and **WS-8**, Figure 1) based on the following considerations: (i) the strong electron-withdrawing properties of benzotriazole to essentially facilitate the electron transfer from the donor to the acceptor/anchor; (ii) a facile structural modification on 2-position in the benzotriazole unit to tailor their solar cell performance; (iii) the absence of sulfur site in benzotriazole, which is prone to form dye-iodine complexes available for serious charge recombination, being probably favorable for high V_{oc};[4c,8] and (iv) like 4-*tert*-butylpyridine (TBP), the nitrogen-containing heterocyclic group of benzotriazole being expectable to improve V_{oc}. Actually, many nitrogen-containing heterocyclic derivatives including imidadole, triazole, pyrimidine, and benzimidazole have been tested as additives in the electrolyte for the sake of increasing V_{oc}.[9] As expected, an improvement in the electron distribution of donor unit in **WS-5** and **WS-8** can be realized, especially in increasing the photostability of synthetic intermediates and final sensitizers. Additionally, the controlled intensity modulated photovoltage spectroscopy was measured to study the effect of alkyl group on V_{oc}. Compared with **WS-8**, the long octyl group introduced to the 2-position of the benzotriazole unit in **WS-5** successfully realized a significant increase in V_{oc} by 100 mV. Charge density data indicate that the two dye-loaded TiO_2 films possess almost the same conduction band position under the same condition. Therefore, the significant enhancement of V_{oc} from methyl to octyl group is attributed to the suppressed charge recombination. With this molecular design, the power conversion efficiency of 8.02% along with a high V_{oc} (0.78 V) was achieved with **WS-5**-based DSSC.

Scheme 1. Synthetic Routes for Sensitizers WS-5 and WS-8[a]

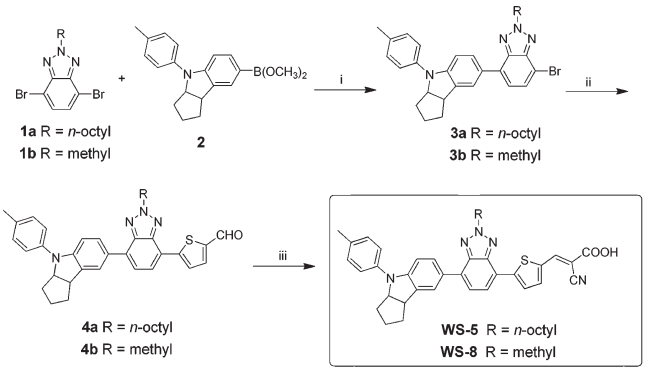

[a] Reaction conditions: (i) $Pd(PPh_3)_4$, 2 M K_2CO_3 aqueous solution, THF, 12 h, 80 °C; (ii) 5-formylthiophen-2-boronic acid, $Pd(PPh_3)_4$, 2 M K_2CO_3 aqueous solution, THF, 12 h, 80 °C; (iii) cyanoacetic acid, piperidine, acetonitrile, 7 h, 80 °C.

EXPERIMENTAL SECTION

Materials. The starting materials of 4,7-dibromo-2-octyl-benzotriazole,[10] 4,7-dibromo-2-methyl-benzotriazole,[11] and 7-bromo-1,2,3,3a,4,8b-hexahydro-4-(4-methylphenyl)-cyclopent[b]indole[12] were synthesized according to the reported literatures. Tetrahydrofuran (THF) was dried over 4 Å molecular sieves and distilled under argon atmosphere from sodium benzophenone ketyl immediately prior to use. All other solvents and chemicals used for synthesis were purchased commercially, and used as received without further purification.

Instrumentation. ^1H NMR and ^{13}C NMR spectra were recorded on a Bruker AM-400 instrument with tetramethylsilane (TMS) as internal standard. High-resolution mass spectroscopy (HRMS) was performed using a Waters LCT Premier XE spectrometer. The UV−vis absorption spectra of the dye solutions and the dye-loaded transparent films were recorded on a Shimadzu UV-3150PC spectrophotometer.

Electrochemical redox potentials were obtained by cyclic voltammetry (CV) measurements, which were performed with a computer-controlled Autolab analyzer using a typical three-electrode electrochemical cell in a solution of tetrabutylammonium hexafluorophosphate (0.1 M) in anhydrous acetonitrile at a scan rate of 50 mV s^{-1} at room temperature under nitrogen. Dye-adsorbed TiO_2 film on conductive glass was used as the working electrode, a Pt wire as the counter electrode, and an Ag/Ag^+ electrode as the reference electrode. The potential of the reference electrode was calibrated with ferrocene, and all potentials mentioned in this work are against the normal hydrogen electrode (NHE).

The electron lifetimes were measured with intensity modulated photovoltage spectroscopy (IMVS),[13] whereas charge densities at open-circuit were measured using charge extraction technique.[14] IMVS and charge extraction analysis were carried out on an electrochemical workstation (Zahner XPOT, Germany), which includes a green light emitting diode (LED, 532 nm) and the corresponding control system. The intensity-modulated spectra were measured at room temperature with light intensity ranging from 0.5 to 45 W/m^2, in modulation frequency ranging from 0.1 Hz to 10 kHz, and with modulation amplitude less than 5% of the light intensity. Charge densities at open circuit under white light from a LED were measured to compare the conduction band positions in different DSSCs.

Synthesis of 3a. Indoline borate **2** (Scheme 1) was prepared with our published method[6a] from the raw material of 7-bromo-1,2,3,3*a*,4,8*b*-hexahydro-4-(4-methylphenyl)-cyclopent[*b*]indole (3.5 g, 10.7 mmol) by a Schlenk technique. The unpurified **2** in THF solution was reacted with 4,7-dibromo-2-octyl-benzotriazole (**1a**, 4.70 g, 12.08 mmol) under

dx.doi.org/10.1021/cm202226j |*Chem. Mater.* 2011, 23, 4394–4401

Suzuki coupling reaction using $Pd(PPh_3)_4$ (0.20 g, 0.17 mmol) and K_2CO_3 aqueous solution (6.0 mL, 2.0 M) as catalysts in THF (25 mL) for 12 h. After cooling, water was added and the reaction mixture was extracted with CH_2Cl_2. The combined organic layer was washed with H_2O and brine, dried over anhydrous Na_2SO_4, and evaporated under reduced pressure. The crude product was purified by column chromatography (CH_2Cl_2/PE = 1/6) on silica gel, and the single substituted product was obtained as a yellow oil **3a** (1.30 g, 2.33 mmol, 19% for two steps). ^{1}H NMR (400 MHz, $CDCl_3$): δ 7.74−7.77 (m, 2 H, phenyl-*H*), 7.57 (d, *J* = 7.7 Hz, 1 H, phenyl-*H*), 7.34 (d, *J* = 7.7 Hz, 1 H, phenyl-*H*), 7.22 (d, *J* = 8.5 Hz, 2 H, phenyl-*H*), 7.16 (d, *J* = 8.4 Hz, 2 H, phenyl-*H*), 6.99 (d, *J* = 8.3 Hz, 1 H, phenyl-*H*), 4.84 (m, 1 H, indoline-C*H*), 4.77 (t, *J* = 7.3 Hz, 2 H, octyl-NCH_2-), 3.91 (m, 1 H, indoline-C*H*), 2.34 (s, 3 H, indoline-CH_3), 2.13 (m, 3 H, octyl-NCH$_2$CH_2- and indoline-CH_2-), 1.95 (m, 2 H, indoline-CH_2-), 1.81 (m, 1 H, indoline-CH_2-), 1.66 (m, 1 H, indoline-CH_2-), 1.59 (m, 1 H, indoline-CH_2-), 1.25 (m, 10 H, octyl-NC$_2$H$_4$C$_5$$H_{10}$-), 0.86 (t, *J* = 6.6 Hz, 3 H, octyl-CH_3). ^{13}C NMR (100 MHz, $CDCl_3$): δ 148.34, 144.42, 142.85, 140.25, 135.40, 131.56, 131.50, 129.78, 129.32, 128.18, 126.52, 124.71, 123.06, 120.20, 107.51, 106.99, 69.23, 56.99, 45.46, 35.15, 33.76, 31.73, 30.19, 29.08, 29.00, 26.59, 24.46, 22.61, 20.80, 14.07. HRMS (ESI, *m*/*z*): $[M]^+$ calcd for $C_{32}H_{37}{}^{79}BrN_4$, 556.2202, $C_{32}H_{37}{}^{81}BrN_4$, 558.2181; found, 556.2205, 558.2196.

Synthesis of 3b. **3b** (0.25 g, 0.54 mmol, yield 20%) was obtained as yellow powder in a similar way with **3a**. ^{1}H NMR (400 MHz, $CDCl_3$): δ 7.71−7.73 (m, 2 H, phenyl-*H*), 7.58 (d, *J* = 7.7 Hz, 1 H, phenyl-*H*), 7.34 (d, *J* = 7.7 Hz, 1 H, phenyl-*H*), 7.22 (d, *J* = 8.5 Hz, 2 H, phenyl-*H*), 7.16 (d, *J* = 8.4 Hz, 2 H, phenyl-*H*), 6.99 (d, *J* = 8.3 Hz, 1 H, phenyl-*H*), 4.83 (m, 1 H, indoline-C*H*), 4.57 (s, 3 H, benzotriazole-CH_3), 3.91 (m, 1 H, indoline-C*H*), 2.34 (s, 3 H, indoline-CH_3), 2.08 (m, 1 H, indoline-CH_2-), 1.94 (m, 2 H, indoline-CH_2-), 1.80 (m, 1 H, indoline-CH_2-), 1.66 (m, 1 H, indoline-CH_2-), 1.59 (m, 1 H, indoline-CH_2-). ^{13}C NMR (100 MHz, $CDCl_3$): δ 148.41, 144.68, 143.14, 140.24, 135.45, 131.60, 131.51, 129.80, 129.52, 128.14, 126.38, 124.72, 123.27, 120.23, 107.55, 106.80, 69.26, 45.45, 43.65, 35.19, 33.76, 24.46, 20.82. HRMS (ESI, *m*/*z*): $[M + H]^+$ calcd for $C_{25}H_{24}{}^{79}BrN_4$, 459.1184, $C_{25}H_{24}{}^{81}BrN_4$, 461.1164; found, 459.1190, 461.1180.

Synthesis of 4a. The mixture of **3a** (0.80 g, 1.43 mmol), 5-formylthiophen-2-boronic acid (0.24 g, 1.54 mmol), $Pd(PPh_3)_4$ (0.16 mg, 0.14 mmol), and K_2CO_3 aqueous solution (6.0 mL, 2.0 M) in THF (35 mL) was refluxed for 12 h under argon. After the solution was cooled, water was added and the reaction mixture was extracted with CH_2Cl_2 three times. The combined organic layer was washed with H_2O and brine, dried over anhydrous Na_2SO_4, and evaporated under reduced pressure. The crude product was purified by column chromatography (CH_2Cl_2/PE = 1/1) on silica gel to obtain the product as a orange red oil **4a** (0.23 g, 0.39 mmol, 27%). ^{1}H NMR (400 MHz, $CDCl_3$): δ 9.94 (s, 1 H, −C*H*O), 8.14 (d, *J* = 4.0 Hz, 1 H, thienyl-*H*), 7.88 (dd, *J* = 8.4 Hz, *J* = 1.6 Hz, 1 H, phenyl-*H*), 7.85 (s, 1 H, phenyl-*H*), 7.78−7.81 (m, 2 H, phenyl-*H* and thienyl-*H*), 7.53 (d, *J* = 7.7 Hz, 1 H, phenyl-*H*), 7.24 (d, *J* = 8.4 Hz, 2 H, phenyl-*H*), 7.18 (d, *J* = 8.3 Hz, 2 H, phenyl-*H*), 7.03 (d, *J* = 8.4 Hz, 1 H, phenyl-*H*), 4.86 (m, 1 H, indoline-C*H*), 4.81 (t, *J* = 7.2 Hz, 2 H, octyl-NCH_2-), 3.93 (m, 1 H, indoline-C*H*), 2.35 (s, 3 H, indoline-CH_3), 2.18 (m, 2 H, octyl-NCH$_2$CH_2-), 2.09 (m, 1 H, indoline-CH_2-), 1.95 (m, 2 H, indoline -CH_2-), 1.81 (m, 1 H, indoline-CH_2-), 1.68 (m, 1 H, indoline-CH_2-), 1.59 (m, 1 H, indoline-CH_2-), 1.40 (m, 4 H, octyl-NC$_2$H$_4$C$_2$$H_4$-), 1.27 (m, 6 H, octyl-NC$_4$H$_8$C$_3$$H_6$-), 0.86 (t, *J* = 5.7 Hz, 3 H, octyl-CH_3). ^{13}C NMR (100 MHz, $CDCl_3$): δ 181.87, 149.37, 147.54, 142.07, 141.37, 140.95, 139.07, 136.32, 134.41, 132.07, 130.66, 128.77, 127.49, 125.78, 125.62, 123.79, 123.73, 121.17, 119.32, 119.27, 106.47, 68.22, 55.82, 44.40, 34.16, 32.68, 30.72, 29.05, 28.08, 27.98, 25.59, 23.42, 21.59, 19.78, 13.04. HRMS (ESI, *m*/*z*): $[M]^+$ calcd for $C_{37}H_{40}N_4OS$, 588.2923; found, 588.2917.

Synthesis of 4b. **4b** (0.08 g, 0.16 mmol, yield 29%) was obtained as orange red powder in a manner similar to that of **4a**. ^{1}H NMR (400 MHz, $CDCl_3$): δ 9.94 (s, 1 H, −C*H*O), 8.13 (d, *J* = 4.0 Hz, 1 H, thienyl -*H*), 7.78−7.85 (m, 4 H, thienyl-*H* and phenyl-*H*), 7.54 (d, *J* = 7.6 Hz, 1 H, phenyl-*H*), 7.24 (d, *J* = 8.4 Hz, 2 H, phenyl-*H*), 7.17 (d, *J* = 8.3 Hz, 2 H, phenyl-*H*), 7.01 (d, *J* = 8.1 Hz, 1 H, phenyl-*H*), 4.86 (m, 1 H, indoline-C*H*), 4.61 (s, 3 H, benzotriazole-CH_3), 3.94 (m, 1 H, indoline-C*H*), 2.35 (s, 3 H, indoline-CH_3), 2.10 (m, 1 H, indoline-CH_2-), 1.94 (m, 2 H, indoline-CH_2-), 1.82 (m, 1 H, indoline-CH_2-), 1.67 (m, 1 H, indoline-CH_2-), 1.60 (m, 1 H, indoline-CH_2-). ^{13}C NMR (100 MHz, $CDCl_3$): δ 181.90, 149.40, 147.51, 141.99, 141.30, 140.91, 139.00, 136.22, 134.39, 132.08, 130.62, 128.80, 127.48, 125.78, 125.64, 123.79, 123.72, 121.15, 119.31, 119.22, 106.45, 68.27, 44.59, 43.71, 34.91, 33.06, 23.91, 20.34. HRMS (ESI, *m*/*z*): $[M + H]^+$ calcd for $C_{30}H_{27}N_4OS$, 491.1906; found, 491.1911.

Synthesis of WS-5. A mixture of aldehyde **4a** (0.27 g, 0.46 mmol) with cyanoacetic acid (43 mg, 0.51 mmol) in acetonitrile (20 mL) was refluxed in the presence of piperidine (0.5 mL) for 7 h under Argon. After cooling the mixture was diluted with CH_2Cl_2, washed by water and brine, dried over Na_2SO_4, and evaporated under reduced pressure. The crude product was purified by column chromatography (CH_2Cl_2/methanol =15/1) on silica gel, and yielded the product as a deep red powder **WS-5** (0.20 g, 0.31 mmol, 67%). ^{1}H NMR (400 MHz, DMSO): δ 8.24 (s, 1 H, =C*H*-), 8.13 (d, *J* = 3.7 Hz, 1 H, thienyl-*H*), 7.73−7.90 (m, 4 H, phenyl-*H* and thienyl-*H*), 7.62 (d, *J* = 7.4 Hz, 1 H, phenyl-*H*), 7.23 (d, *J* = 7.7 Hz, 2 H, phenyl-*H*), 7.18 (d, *J* = 7.7 Hz, 2 H, phenyl-*H*), 6.93 (d, *J* = 8.3 Hz, 1 H, phenyl-*H*), 4.89 (m, 1 H, indoline-C*H*), 4.81 (t, *J* = 7.2 Hz, 2 H, octyl-NCH_2-), 3.88 (m, 1H, indoline-C*H*), 2.29 (s, 3 H, indoline-CH_3), 2.06 (m, 3 H, octyl-NCH$_2$CH_2- and indoline-CH_2-), 1.76−1.82 (m, 3 H, indoline-CH_2-), 1.62 (m, 1 H, indoline-CH_2-), 1.40 (m, 1 H, indoline-CH_2-), 1.19 (m, 4 H, octyl-NC$_2$H$_4$C$_2$$H_4$-),1.30 (m, 6 H, octyl-NC$_4$H$_8$C$_3$$H_6$-), 0.78 (t, *J* = 5.7 Hz, 3 H, octyl-CH_3). ^{13}C NMR (100 MHz, DMSO): δ 163.89, 147.59, 145.01, 142.15, 141.53, 141.35, 139.46, 136.21, 136.10, 135.13, 130.94, 130.84, 129.73, 128.11, 126.88, 126.02, 124.39, 124.06, 122.08, 119.86, 119.62, 118.79, 106.88, 68.30, 56.17, 44.59, 34.85, 33.09, 31.10, 29.15, 28.44, 28.22, 25.86, 23.93, 21.99, 20.37, 13.84. HRMS (ESI, *m*/*z*): $[M + H]^+$ calcd for $C_{40}H_{42}N_5O_2S$, 656.3059; found, 656.3058.

Synthesis of WS-8. **WS-8** (60 mg, 0.11 mmol, yield 68%) was obtained as deep red powder in similar way with **WS-5**: ^{1}H NMR (400 MHz, DMSO): δ 13.83 (br, 1 H, −COO*H*), 8.46 (s, 1 H, =C*H*-), 8.18 (d, *J* = 3.4 Hz, 1 H, thienyl-*H*), 8.04 (d, *J* = 3.3 Hz, 1 H, thienyl-*H*), 7.90−7.94 (m, 3 H, phenyl-*H*), 7.68 (d, *J* = 7.6 Hz, 1 H, phenyl-*H*), 7.24 (d, *J* = 8.0 Hz, 2 H, phenyl-*H*), 7.19 (d, *J* = 8.0 Hz, 2 H, phenyl-*H*), 6.95 (d, *J* = 8.2 Hz, 1 H, phenyl-*H*), 4.90 (m, 1 H, indoline-C*H*), 4.61 (s, 3 H, benzotriazole-CH_3), 3.90 (m, 1 H, indoline-C*H*), 2.29 (s, 3 H, indoline-CH_3), 2.08 (m, 1 H, indoline-CH_2-), 1.85 (m, 3 H, indoline-CH_2-), 1.63 (m, 1 H, indoline-CH_2-), 1.42 (m, 1 H, indoline-CH_2-). ^{13}C NMR (100 MHz, DMSO): δ 163.70, 148.14, 147.78, 145.66, 142.37, 141.74, 139.92, 139.40, 135.21, 135.10, 131.59, 130.95, 129.76, 128.30, 126.94, 125.83, 124.86, 124.46, 122.10, 119.73, 119.25, 116.90, 115.79, 106.91, 68.36, 44.57, 43.72, 34.91, 33.07, 23.94, 20.37. (ESI, *m*/*z*): $[M + H]^+$ calcd for $C_{33}H_{28}N_5O_2S$, 558.1964; found, 558.1962.

Fabrication of Dye-Sensitized Solar Cells. Fluorine-doped SnO_2 glass (15 Ω/sq, transmittance 80−85%, Nippon Sheet Glass, Japan) substrates were cleaned in a detergent solution by an ultrasonic bath, washed with acetone and water, and then dried using N_2 current. Nanocrystalline TiO_2 films, 14 μm, consisting of a 7 μm transparent layer (~ 20 nm nanoparticles) and 7 μm scattering layer (~ 100 nm particles)[15] in thickness, were prepared using a screen printing technique, followed by sintering at 525 °C under an air flow. After cooling, the TiO_2 films were impregnated in a 0.05 M aqueous $TiCl_4$ solution for 30 min at 70 °C, and then rinsed with deionized water. The $TiCl_4$-treated TiO_2 films were annealed at 450 °C for 30 min, and then cooled to 120 °C before immersed into the dye solution (0.3 mM in chloroform:ethanol = 3:7) for 16 h to allow the dye molecules to adsorb onto

the TiO_2 surface. After the adsorption of dyes, the electrodes were rinsed with chloroform and acetonitrile, respectively. The resulting photoelectrode and the Pt-counter electrode were assembled into a sealed sandwich solar cell with a thermoplastic frame (Surlyn 30 μm thick). Redox electrolyte (0.6 M 1,2-dimethyl-3-*n*-propylimidazolium iodide, 0.1 M LiI, 0.05 M I_2, and 0.5 M 4-*tert*-butylpyridine in acetonitrile) was introduced through a hole in the counter electrode via suction through another drilled hole. Finally, the two holes were sealed using another hot melt Surlyn film covered with a thin glass slide.[16]

Photovoltaic Measurements. The current density−voltage ($J-V$) characteristics of the DSSCs were measured by recording $J-V$ curves using a Keithley 2400 source meter under the illumination of AM1.5G simulated solar light coming from an AAA solar simulator (Newport-94043A equipped with a 450 W Xe lamp and an AM1.5G filter). The DSSCs were fully covered with a black mask with an aperture area of 0.2304 cm^2 during measurements. The incident light intensity was calibrated with a standard silicon solar cell (Newport 91150). Action spectra of the incident monochromatic photon-to-electron conversion efficiency (IPCE) for the solar cells were obtained with an Oriel-74125 system (Oriel Instruments). The intensity of monochromatic light was measured with a Si detector (Oriel-71640).

RESULTS AND DISCUSSION

Design and Synthesis. In D−π−A configuration of sensitizers, the tuning of donor and acceptor units has been well demonstrated to extend the absorption spectrum, adjust the HOMO and LUMO levels, and realize the intramolecular charge separation. As well demonstrated, the indoline unit has more powerful electron-donating capability than that of common triphenylamine.[6a,e] As shown in Figure 1, for the design of sensitizers **WS-5** and **WS-8**, we employed indoline unit as the donor, cyanoacetic acid as the acceptor/anchor, and a thiophene moiety as the conjugation bridge. Additionally, an electron-withdrawing benzotriazole unit was incorporated between the donor and π-conjugation unit. We have demonstrated that the additional acceptor unit can facilitate the electron migration from the donor to the cyanoacetic acetic unit.[6a,d] However, the V_{oc} is relatively low as compared to the reported efficient DSSCs. Considering that 4-*tert*-butylpyridine (TBP), imidadole, pyrimidine and benzimidazole have been employed as additives in the electrolyte to increase V_{oc}, here the nitrogen-containing heterocyclic group of benzotriazole unit can be expectable to enhance V_{oc}. As well-known, the strong intermolecular $\pi-\pi$ interaction may lead to interfacial charge recombination, thus resulting in a decrease in V_{oc}. To reduce the intermolecular $\pi-\pi$ interaction, an alkyl group was conveniently linked to the 2-position of benzotriazole unit. As depicted in Scheme 1, the syntheses of **WS-5** and **WS-8** were started from 4,7-dibromo-2-methyl-benzotriazole and 4,7-dibromo-2-octyl-benzotriazole, respectively.[10,11] Two asymmetrical Suzuki coupling[17] with indoline borate **2** and 5-formylthiophen-2-boronic acid, respectively, afforded monoaldehyde-substituted precursors **4a** and **4b**. Because of the low oxidation potential, the bromo-substituted indoline was extremely photosensitive and deteriorated in a short time under day light and air with color change from very pale yellow to dark green. We checked the deteriorated chemical with traditional thin layer chromatography, showing at least two new byproduct components. By contrast, after connecting the electron-withdrawing acceptor unit of benzotriazole group, the resulting indoline intermediates became very stable for half a year without distinct color change. Therefore, the design of D−A−π−A configuration is beneficial to not only the synthetic process, but also the photostability in the DSSC operation. Finally, the obtained precursors were converted to sensitizers **WS-5** and **WS-8** by Knoevenagel condensation[18] with cyanoacetic acid by reflux in acetonitrile in the presence of piperidine, which were well characterized by ^1H NMR, ^{13}C NMR, and HRMS. The obtained dyes are deep red in solid state, and can be dissolved in dichloromethane, THF, and toluene.

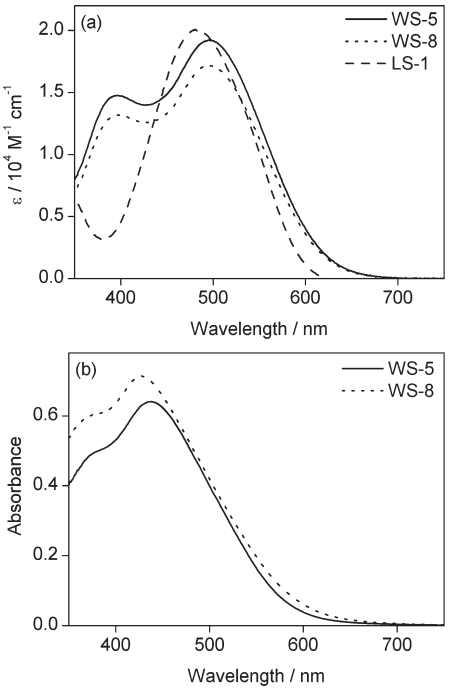

Figure 2. (a) Absorption spectra of **WS-5**, **WS-8**, and reference **LS-1** in CH_2Cl_2 solutions. (b) Absorption spectra of **WS-5** and **WS-8** anchored onto TiO_2 films (1.0 μm in thickness).

Table 1. Photophysical and Electrochemical Properties of Sensitizers WS-5 and WS-8

	absorption					
dye	λ_{max} (nm) [a]	ε (M^{-1} cm^{-1}) [a]	λ_{max} on TiO_2 (nm)	HOMO (V) [b]	E_{0-0} (eV) [c]	LUMO (V) [d]
WS-5	496	19200	438	0.94	2.12	−1.18
WS-8	495	17200	428	0.92	2.09	−1.17

[a] Absorption peaks (λ_{max}) and molar extinction coefficients (ε) were measured in CH_2Cl_2 ($\sim 1 \times 10^{-5}$ M). [b] The formal oxidation potentials (vs NHE) in acetonitrile were internally calibrated with ferrocene, and taken as the HOMO. [c] E_{0-0} was estimated from the wavelength at 10% maximum absorption intensity for the dye-loaded TiO_2 film. [d] The LUMO was calculated with the expression of LUMO = HOMO − E_{0-0}.

UV−Vis Absorption Properties. The UV−vis absorption spectra of two sensitizers in CH_2Cl_2 solutions (1×10^{-5} M) are shown in Figure 2a, and the corresponding properties are summarized in Table 1. The absorption spectra of dyes **WS-5** and **WS-8** display the maximum absorption wavelength at 496 (ε = 1.92×10^4 M^{-1} cm^{-1}) and 495 nm ($\varepsilon = 1.72 \times 10^4$ M^{-1} cm^{-1}), respectively, due to the intramolecular charge transfer (ICT) from the donor to the acceptor. The almost identical absorption maxima and extinction coefficients are not difficult to be

dx.doi.org/10.1021/cm202226j |*Chem. Mater.* 2011, 23, 4394–4401

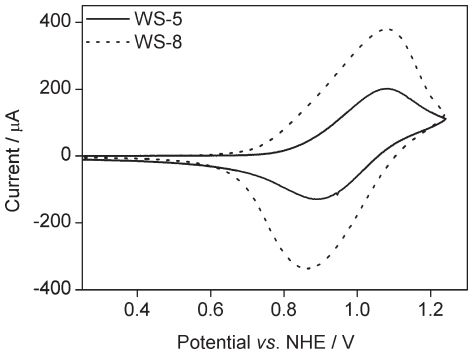

Figure 3. Cyclic voltammograms of the dye-loaded TiO_2 films (6 μm thick, 0.25 cm^2 in area) for **WS-5** and **WS-8**. Note that the current intensity of **WS-5** is decreased by around 50% with respect to **WS-8**.

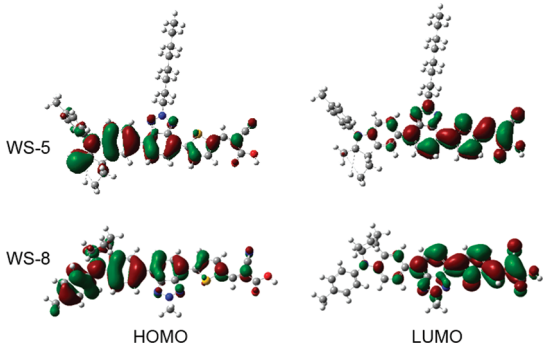

Figure 4. Frontier orbitals of **WS-5** and **WS-8**.

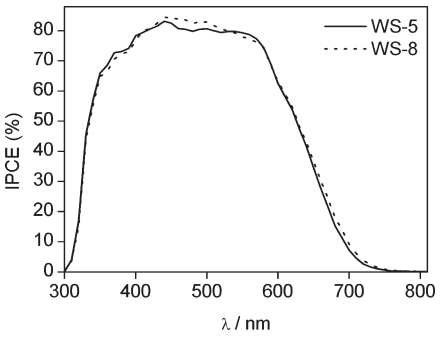

Figure 5. IPCE action spectra for DSSCs based on **WS-5** and **WS-8**.

understood as **WS-5** and **WS-8** have similar chemical structures except for the alkyl chain length attached at the benzotriazole unit. Compared with reference dye **LS-1** (Figure 1) whose absorption peak is located at 483 nm ($2.01 \times 10^4\ M^{-1}\ cm^{-1}$), the introduction of benzotriazole unit into the molecular frame can redshift the ICT absorption peak by 12−13 nm (Figure 2a). Moreover, in **WS-5** and **WS-8**, the additional absorption band appearing at around 400 nm and the apparent red-shift in the absorption threshold are beneficial to the light harvesting. Consequently, the benzotriazole unit can efficiently decrease the band gap and optimize energy levels, thus resulting in the longer responsive wavelength region and higher light-harvesting efficiency.

Figure 2b shows the absorption spectra of the organic sensitizers anchored onto a transparent nanocrystalline TiO_2 film (1.0 μm). After adsorption onto the TiO_2 films, **WS-5** and **WS-8** exhibit absorption peaks hypsochromically shifted to 438 and 428 nm, respectively, which is mainly ascribed to the deprotonation of the carboxylic acid and the different polarity of medium.[19] Compared with the hypsochromic shift of 58 nm for **WS-5**, the hypsochromic shift for **WS-8** is more remarkable (67 nm), probably due to the stronger $\pi-\pi$ interaction in **WS-8** than in **WS-5** because the longer alkyl chain can weaken the $\pi-\pi$ interaction. Furthermore, the absorption intensity of **WS-5** loaded TiO_2 film is slightly lower than that for **WS-8**. Obviously, the lower dye adsorption amount for **WS-5** on TiO_2 surface stems from the larger molecular size and weaker intermolecular $\pi-\pi$ interaction of **WS-5** with octyl group than **WS-8** with methyl group. This is further proven by desorbing organic dyes from the TiO_2 surface. The surface concentration of **WS-5** is 4.7×10^{-8} mol cm^{-2} μm^{-1}, whereas that for **WS-8** increased to 5.5×10^{-8} mol cm^{-2} μm^{-1}.

Electrochemical Properties. To investigate the oxidation potential of organic dyes and thermodynamically evaluate the possibility of sensitizer regeneration, cyclic voltammetry was carried out in a typical three-electrode electrochemical cell with TiO_2 films stained with sensitizer as the working electrode (Figure 3). The formal oxidation potentials, taken as the HOMO levels of sensitizers **WS-5** and **WS-8**, are calculated to be 0.94 and 0.92 V (vs. NHE, same below), respectively, which are more positive than I^-/I_3^- redox couples (~ 0.4 V), indicating that the reduction of oxidized dyes with I^- ions is thermodynamically feasible. Correspondingly, estimated from the band gap[5e] derived from the wavelength at 10% maximum absorption intensity for the dye-loaded TiO_2 film, the LUMO levels of **WS-5** and **WS-8** are calculated to be −1.18 and −1.17 V, respectively, indicating a sufficient driving force for electron injection from oxidized organic dyes to TiO_2 films.[20] The energy levels for the two dyes are also listed in Table 1.

It should be noted that the current intensity of **WS-5** is decreased by around 50% with respect to **WS-8** (Figure 3), which is much higher than the absorption decrease from **WS-8** to **WS-5** (by 10%). It is suggestive that the decreased adsorption amount cannot be the only cause for the decreased current intensity. As we have discussed elsewhere,[21] the initial oxidation of dye molecules followed by intermolecular electron hopping across the TiO_2 nanoparticle surface is one accepted mechanism for charge transfer in working electrode.[22] Therefore, the formation of $\pi-\pi$ stacking in **WS-8** allows facile intermolecular electron hopping as evidenced by the strong current signal. Upon the incorporation of octyl group in **WS-5**, the long alkyl chain suppresses the intermolecular interaction among the dye molecules, which results in the weakened electron hopping between each other and the significant decrease in current intensity.

Theoretical Approach. To gain insight into the geometrical and electronic properties of the resulted sensitizers, density functional calculations were conducted using the Gaussian 03 program package at the B3LYP/6-31G* level. It is clearly seen from Figure 4 that the HOMO is distributed along the D−A−π system and the LUMO is evenly delocalized across the entire A−π−A system. The well-overlapped HOMO and LUMO orbitals on the benzotriazole unit indirectly suggest the well inductive or withdrawing electron tendency from indoline donor unit to the cyanoacetic acid unit. After photoexcitation, the electrons in the organic dyes loaded on nanocrystalline TiO_2 surface could be successively transferred from the donor to the benzotriazole unit, and then transferred to the cyanoacetic acid

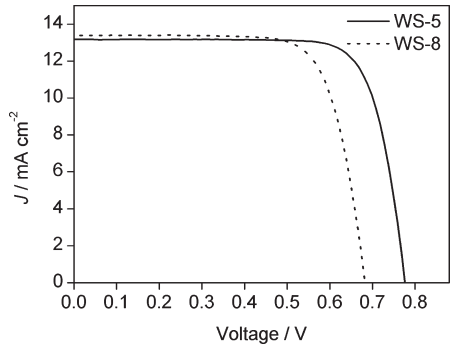

Figure 6. $J-V$ characteristics of DSSCs based on **WS-5** and **WS-8** measured under illumination of simulated AM1.5G solar light (100 mW cm^{-2}).

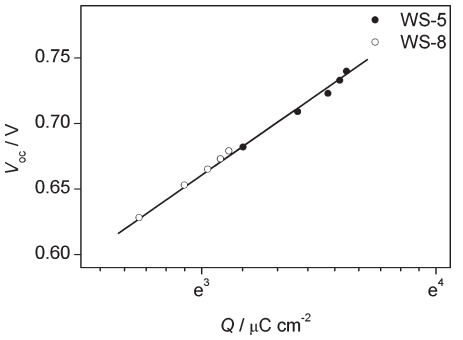

Figure 7. Charge density at open circuit as a function of V_{oc} for DSSCs with **WS-5** and **WS-8**. Three identical devices were tested in each case with standard deviation less than 1%.

subunit, and finally into TiO_2. The well-delocalized LUMO over the A−π−A units indicates that the additional acceptor of benzotriazole unit could facilitate the electron transfer from the donor to the acceptor/anchor (i.e. cyanoacetic unit).

Solar Cell Performance. Figure 5 shows the IPCE action spectra of the DSSCs based on sensitizers **WS-5** and **WS-8**. The onsets of IPCE for both dyes are above 700 nm, which are consistent with the absorption onsets in the magnified absorption spectra (Figure 2b). It can be found that both **WS-5** and **WS-8** based DSSCs display a platform in the spectral range of 400 − 580 nm with maximum IPCE over 80%. Taking the reflectance and absorption by the conductive glass into account, the maximum IPCE can be regarded as unity. Without coadsorption, the two dyes exhibit efficient photoelectric conversion, in contrast to our previously reported dye **WS-2**, which produces maximum IPCE below 60% without coadsorption and above 80% with coadsorption.[6a]

The current density−voltage ($J-V$) curves of the DSSCs based on **WS-5** and **WS-8** under simulated AM1.5G irradiation (100 mW cm^{-2}) are displayed in Figure 6, where short-circuit photocurrent (J_{sc}), open-circuit photovoltage (V_{oc}), fill factor (FF), and power conversion efficiency (η) can be determined. The DSSC based on **WS-8** produces η of 6.74% (J_{sc} = 13.39 mA cm^{-2}, V_{oc} = 0.68 V, FF = 0.74). We previously reported a benzothiadiazole dye (**WS-2**),[6a] which produced η of 5.35% (J_{sc} = 12.90 mA cm^{-2}, V_{oc} = 0.61 V, FF = 0.68) under the same condition. Evidently, **WS-8** is better in terms of solar cell performance, especially in V_{oc}, than **WS-2** without coadsorption. Although V_{oc} of **WS-2** based DSSC was improved to 0.65 V with coadsorption, it was still lower than that of **WS-8** based DSSC without coadsorption. When a hexyl group was linked to the thiophene unit in **WS-2**, the obtained V_{oc} of 0.67 V was much lower than that (0.78 V) for **WS-5**. These results indicate that incorporation of benzotriazole unit into the dye skeleton is advantageous to high V_{oc}. Actually, many nitrogen-containing heterocyclic derivatives including 4-*tert*-butylpyridine (TBP), imidadole, triazole, pyrimidine, and benzimidazole have been tested as additives in the electrolyte for the sake of increasing V_{oc}.[9] Here, considering the very similar configuration between **WS-2** and **WS-8**, the incorporated nitrogen-containing heterocyclic group of benzotriazole in **WS-8** would be responsible for the increased V_{oc}. Additionally, because it is considered that sulfur atom is prone to form dye−iodine complexes available for serious charge recombination,[8] the absence of sulfur atom in benzotriazole unit for **WS-8** with respect to the benzothiadiazole for **WS-2** might be beneficial to an increase in electron lifetime, which lacks evidence so far and needs to be investigated in the future. The detailed reasons why **WS-8** generates higher V_{oc} than **WS-2** will be clarified in another research. When the methyl group in dye **WS-8** is replaced with octyl group (**WS-5**), a significant enhancement of V_{oc}, a mild increase in FF, and similar J_{sc} are observed. As a result, η of 8.02% (J_{sc} = 13.18 mA cm^{-2}, V_{oc} = 0.78 V, FF = 0.78) was achieved for **WS-5** based DSSC. Many cells were tested for the two dyes, and always **WS-5** based DSSC produces higher η and V_{oc} than **WS-8**-based DSSC.

Remarkably, the distinct enhancement of V_{oc} from short methyl group to octyl chain is realized in this work. The V_{oc} for **WS-5** (0.78 V) is much higher than that (0.67 V) for the benzothiadiazole dye with a long alkyl chain under the same condition. This suggests that the incorporation of benzotriazole unit into the dye might be expectable to overcome the major limitation to the relatively low V_{oc} for metal-free DSSCs.

The generation of V_{oc} is related to the conduction band position of TiO_2 and the charge recombination rate in DSSCs. To understand the significant improvement of the V_{oc} from **WS-8** to **WS-5**-based DSSC, first, the relative conduction band position in the DSSCs based on **WS-5** and **WS-8** was investigated. According to the method developed by Frank and coworkers,[23] the movement of conduction band contributes to the change in V_{oc} at constant photoinduced charge density (Q) which was measured with charge extraction technique[14] under illumination of a white light from LED. Three identical devices were tested in each case with standard deviation less than 1%. Figure 7 displays the charge density at open circuit as a function of V_{oc} for DSSCs with **WS-5** or **WS-8**. It can be found that for both DSSCs based on **WS-5** and **WS-8**, the V_{oc} increases linearly with the logarithm of Q. The two curves for the corresponding DSSCs have the same slope (125 mV) and coincide with each other. At fixed Q, the almost same V_{oc} for both DSSCs indicates the identical conduction band position for two cases. Therefore, the conduction band edge is not influenced when the alkyl in benzotriazole is changed from methyl to octyl.

Because the introduction of a longer alkyl chain into the dye molecule does not induce the movement of the conduction band of TiO_2, the significant improvement of V_{oc} from **WS-8** to **WS-5** based DSSC should be attributed to the repression of charge recombination, which is related to electron lifetime (τ). Figure 8 shows the electron lifetime as a function of charge density at open circuit for the DSSCs based on **WS-5** and **WS-8**, respectively. The electron lifetime was obtained from the frequency at the top

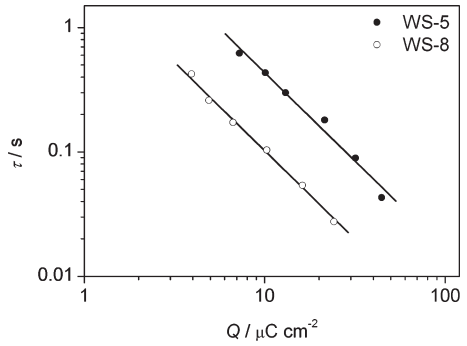

Figure 8. Electron lifetime as a function of charge density at open circuit. Electron lifetime was measured with IMVS under different intensities of a 532 nm light from LED, and charge densities were measured with charge extraction technique under the same light intensities for IMVS measurement. Three identical cells were tested in each case with standard deviation less than 4%.

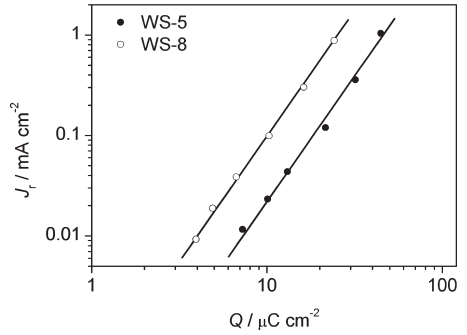

Figure 9. Charge recombination current as a function of charge density at open circuit. Q was measured under illumination of a 532 nm light from LED. J_{sc} measured at the same light intensity for Q measurement was approximately taken as J_r because of the negligible charge recombination at short circuit. Three identical cells were tested in each case with standard deviation less than 5%.

of the semicircle (f_{min}) in IMVS by the relation $\tau = (2\pi f_{min})^{-1}$. The charge density at open circuit under the same light intensity for IMVS measurement was obtained from charge extraction. Three identical cells were tested in each case with standard deviation less than 4%. As shown in Figure 8, the electron lifetime decreases with charge density following a power law relation with the same slope, suggesting the same recombination mechanism. At a fixed charge density, the electron lifetime for the DSSC based on **WS-5** is larger than that of **WS-8** based DSSC by around 4-fold. The long octyl group is more effective than the short methyl group to block I_3^- ions (or iodine) approaching the TiO_2 surface for charge recombination, and thus **WS-5** shows much longer electron lifetime than **WS-8**.

Finally, to analyze the effect of alkyl chains on charge recombination rate, charge recombination current (J_r) at open circuit is plotted against charge density (Q, Figure 9). At open circuit and a fixed light intensity, the recombination current density J_r equals the charge-injection current density. However, neither of them can be directly measured, but can be estimated from the measurement of J_{sc}. At short-circuit, J_r is taken as J_{sc} in value under the same light intensity because of the negligible charge recombination.[23] It is evident from Figure 9 that the recombination current for both cases increases with Q following a power law relation with the same exponent of 2.5. Again, the same slope or exponent suggests the same recombination mechanism for both DSSCs. Moreover, at fixed Q, J_r for **WS-8**-based DSSC is about 4 times larger than that for **WS-5** based DSSC, indicating that the recombination rate constant is thus reduced by 4-fold when methyl is replaced with octyl group. The retarded charge recombination rate constant will reduce current or electron loss at open circuit. When more charge is accumulated in TiO_2, Fermi level moves upward and V_{oc} gets larger. The measured charge density at open circuit under one sun illumination for **WS-5** is about 2-fold higher than that for **WS-8**. According to the relation of $Q-V_{oc}$ (Figure 7), the V_{oc} gain arising from the increased Q is calculated to be about 90 mV, explaining why **WS-5** based DSSC produces 100 mV higher V_{oc} than the **WS-8**-based DSSC.

CONCLUSIONS

In summary, we have successfully designed and synthesized two novel benzotriazole-containing organic sensitizers with D−A−π−A configuration. Replacing the methyl group with octyl group does not bring about significant changes in absorption spectrum and energy levels. However, the octyl group suppresses charge recombination rate constant by 4-fold as compared to the methyl group. As a result, without any coadsorption, **WS-5**-based DSSC achieved η of 8.02% with V_{oc} higher than **WS-8** by 100 mV. Because of incorporation of benzotriazole unit into the dye skeleton, V_{oc} as high as 0.78 V was obtained. Our studies clearly demonstrate the relation between molecular structure and device performance. These findings will pave a new way to design new efficient dye sensitizers.

ASSOCIATED CONTENT

Supporting Information. Discussion on the low yields of the Suzuki coupling reaction using 5-formylthiophen-2-boronic acid and characterization of the sensitizers **WS-5** and **WS-8** by ^{1}H NMR, ^{13}C NMR, and HRMS. This material is available free of charge via the Internet at http://pubs.acs.org.

AUTHOR INFORMATION

Corresponding Author

*E-mail: zhougang@fudan.edu.cn; zs.wang@fudan.edu.cn. Fax: (+86)21-5163-0345; whzhu@ecust.edu.cn. Fax: (+86)21-6425-2758.

Author Contributions

†These authors contributed equally to this work.

ACKNOWLEDGMENT

This work was financially supported by the National Basic Research Program (2011CB933302) of China, the National Natural Science Foundation of China (20971025, 90922004, and 50903020), the Shanghai nongovernmental international cooperation program (10530705300), Shanghai Leading Academic Discipline Project (B108), the Oriental Scholarship, the Fundamental Research Funds for the Central Universities (WK1013002), and Jiangsu Major Program (BY2010147).

REFERENCES

(1) O'Regan, B.; Grätzel, M. *Nature* **1991**, *353*, 737–740.

(2) (a) Kim, S.; Lee, J. K.; Kang, S. O.; Ko, J.; Yum, J. H.; Fantacci, S.; De Angelis, F.; Di Censo, D.; Nazeeruddin, M. K.; Grätzel, M. *J. Am. Chem. Soc.* **2006**, *128*, 16701–16707. (b) Choi, H.; Baik, C.; Kang, S. O.; Ko, J.; Kang, M. S.; Nazeeruddin, M. K.; Grätzel, M. *Angew. Chem., Int. Ed.* **2008**, *47*, 327–330. (c) Ito, S.; Miura, H.; Uchida, S.; Takata, M.; Sumioka, K.; Liska, P.; Comte, P.; Pechy, P.; Grätzel, M. *Chem. Commun.* **2008**, 5194–5196. (d) Kim, S.; Kim, D.; Choi, H.; Kang, M. S.; Song, K.; Kang, S. O.; Ko, J. *Chem. Commun.* **2008**, 4951–4593. (e) Wang, Z.-S.; Koumura, N.; Cui, Y.; Takahashi, M.; Sekiguchi, H.; Mori, A.; Kubo, T.; Furube, A.; Hara, K. *Chem. Mater.* **2008**, *20*, 3993–4003. (f) Xu, M. F.; Wenger, S.; Bala, H.; Shi, D.; Li, R. Z.; Zhou, Y. Z.; Zakeeruddin, S. M.; Grätzel, M.; Wang, P. *J. Phys. Chem. C* **2009**, *113*, 2966–2973. (g) Zhang, G.; Bala, H.; Cheng, Y.; Shi, D.; Lv, X.; Yu, Q.; Wang, P. *Chem. Commun.* **2009**, 2198–2200. (h) Choi, H.; Raabe, I.; Kim, D.; Teocoli, F.; Kim, C.; Song, K.; Yum, J.-H.; Ko, J.; Nazeeruddin, M. K.; Grätzel, M. *Chem.—Eur. J.* **2010**, *16*, 1193–1201. (i) Zeng, W.; Cao, Y.; Bai, Y.; Wang, Y.; Shi, Y.; Zhang, M.; Wang, F.; Pan, C.; Wang, P. *Chem. Mater.* **2010**, *22*, 1915–1925.

(3) (a) Nazeeruddin, M. K.; De Angelis, F.; Fantacci, S.; Selloni, A.; Viscardi, G.; Liska, P.; Ito, S.; Takeru, B.; Grätzel, M. *J. Am. Chem. Soc.* **2005**, *127*, 16835–16847. (b) Grätzel, M. *J. Photochem. Photobiol. C* **2003**, *4*, 145–153. (c) Gao, F.; Wang, Y.; Shi, D.; Zhang, J.; Wang, M.; Jing, X.; Humphry-Baker, R.; Wang, P.; Zakeeruddin, S. M.; Grätzel, M. *J. Am. Chem. Soc.* **2008**, *130*, 10720–10728. (d) Chen, C.-Y.; Wang, M.; Li, J.-Y.; Pootrakulchote, N.; Alibabaei, L.; Ngoc-le, C.-H.; Decoppet, J.-D.; Tsai, J.-H.; Grätzel, C.; Wu, C.-G.; Zakeeruddin, S. M.; Grätzel, M. *ACS Nano* **2009**, *3*, 3103–3109. (e) Chiba, Y.; Islam, A.; Watanabe, Y.; Komiya, R.; Koide, N.; Han, L. Y. *Jpn. J. Appl. Phys., Part 2* **2006**, *45*, L638–L640. (f) Peic, A.; Staff, D.; Risbridger, T.; Menges, B.; Peter, L. M.; Walker, A. B.; Cameron, P. J. *J. Phys. Chem. C* **2011**, *115*, 613–619.

(4) (a) Mishra, A.; Fischer, M. K. R.; Bauerle, P. *Angew. Chem., Int. Ed.* **2009**, *48*, 2474–2499. (b) Hagfeldt, A.; Boschloo, G.; Sun, L.; Kloo, L.; Pettersson, H. *Chem. Rev.* **2010**, *110*, 6595–6663. (c) Ning, Z.; Fu, Y.; Tian, H. *Energy Environ. Sci.* **2010**, *3*, 1170–1181.

(5) (a) Hara, K.; Sato, T.; Katoh, R.; Furube, A.; Ohga, Y.; Shinpo, A.; Suga, S.; Sayama, K.; Sugihara, H.; Arakawa, H. *J. Phys. Chem. B* **2003**, *107*, 597–606. (b) Sayama, K.; Tsukagoshi, S.; Hara, K.; Ohga, Y.; Shinpou, A.; Abe, Y.; Suga, S.; Arakawa, H. *J. Phys. Chem. B* **2002**, *106*, 1363–1371. (c) Miyashita, M.; Sunahara, K.; Nishikawa, T.; Uemura, Y.; Koumura, N.; Hara, K.; Mori, A.; Abe, T.; Suzuki, E.; Mori, S. *J. Am. Chem. Soc.* **2008**, *130*, 17874–17881.

(6) (a) Zhu, W. H.; Wu, Y. Z.; Wang, S. T.; Li, W. Q.; Li, X.; Chen, J. A.; Wang, Z.-S.; Tian, H. *Adv. Funct. Mater.* **2011**, *21*, 756–763. (b) Velusamy, M.; Thomas, K. R. J.; Lin, J. T.; Hsu, Y. C.; Ho, K. C. *Org. Lett.* **2005**, *7*, 1899–1902. (c) Chang, D. W.; Lee, H. J.; Kim, J. H.; Park, S. Y.; Park, S.-M.; Dai, L.; Baek, J.-B. *Org. Lett.* **2011**, *13*, 3880–3883. (d) Wang, Z.-S.; Cui, Y.; Hara, K.; Dan-oh, Y.; Kasada, C.; Shinpo, A. *Adv. Mater.* **2007**, *19*, 1138–1141. (e) Liu, B.; Zhu, W. H.; Zhang, Q.; Wu, W. J.; Xu, M.; Ning, Z. J.; Xie, Y. S.; Tian, H. *Chem. Commun.* **2009**, 1766–1768.

(7) (a) Zhang, L.; He, C.; Chen, J.; Yuan, P.; Huang, L.; Zhang, C.; Cai, W.; Liu, Z.; Cao, Y. *Macromolecules* **2010**, *43*, 9771–9778. (b) Li, C.; Liu, M.; Pschirer, N. G.; Baumgarten, M.; Müllen, K. *Chem. Rev.* **2010**, *110*, 6817–6855.

(8) (a) Zhang, M.; Liu, J.; Wang, Y.; Zhou, D.; Wang, P. *Chem. Sci.* **2011**, *2*, 1401–1406. (b) O'Regan, B. C.; Walley, K.; Juozapavicius, M.; Anderson, A.; Matar, F.; Ghaddar, T.; Zakeeruddin, S. M.; Klein, C.; Durrant, J. R. *J. Am. Chem. Soc.* **2009**, *131*, 3541–3548.

(9) (a) Kusama, H.; Arakawa, H. *J. Photochem. Photobiol., A* **2004**, *164*, 103–110. (b) Kusama, H.; Arakawa, H. *J. Photochem. Photobiol., A* **2004**, *162*, 441–448. (c) Nakade, S.; Kanzaki, T.; Kubo, W.; Kitamura, T.; Wada, Y.; Yanagida, S. *J. Phys. Chem. B* **2005**, *109*, 3480–3487.

(10) Tanimoto, A.; Yamamoto, T. *Macromolecules* **2006**, *39*, 3546–3552.

(11) Le, Z. G.; Chen, Z. C.; Hu, Y.; Zheng, Q. G. *J. Chem. Res.* **2004**, *5*, 344–346.

(12) Miyata, O.; Takeda, N.; Kimura, Y.; Takemoto, Y.; Tohnai, N.; Miyata, M.; Naito, T. *Tetrahedron* **2006**, *62*, 3629–3647.

(13) Schlichthörl, G.; Huang, S. Y.; Sprague, J.; Frank, A. J. *J. Phys. Chem. B* **1997**, *101*, 8141–8155.

(14) Duffy, N. W.; Peter, L. M.; Rajapakse, R. M. G.; Wijayantha, K. G. U. *J. Phys. Chem. B* **2000**, *104*, 8916–8919.

(15) Wang, Z.-S.; Kawauchi, H.; Kashima, T.; Arakawa, H. *Coord. Chem. Rev.* **2004**, *248*, 1381–1389.

(16) Wang, Z.-S.; Yamaguchi, T.; Sugihara, H.; Arakawa, H. *Langmuir* **2005**, *21*, 4272–4276.

(17) Miyaura, N.; Suzuki, A. *Chem. Rev.* **1995**, *95*, 2457–2483.

(18) Knoevenagel, E. *Ber. Deutsch. Chem. Gesell.* **1898**, *31*, 2596–2619.

(19) (a) Hara, K.; Wang, Z.-S.; Sato, T.; Furube, A.; Katoh, R.; Sugihara, H.; Dan-oh, Y.; Kasada, C.; Shinpo, A.; Suga, S. *J. Phys. Chem. B* **2005**, *109*, 15476–15482. (b) Thomas, K. R. J.; Hsu, Y. C.; Lin, J. T.; Lee, K. M.; Ho, K. C.; Lai, C. H.; Cheng, Y. M.; Chou, P. T. *Chem. Mater.* **2008**, *20*, 1830–1840. (c) Hagberg, D. P.; Edvinsson, T.; Marinado, T.; Boschloo, G.; Hagfeldt, A.; Sun, L. *Chem. Commun.* **2006**, 2245–2247. (d) Li, S.-L.; Jiang, K.-J.; Shao, K.-F.; Yang, L.-M. *Chem. Commun.* **2006**, 2792–2794. (e) Koumura, N.; Wang, Z.-S.; Mori, S.; Miyashita, M.; Suzuki, E.; Hara, K. *J. Am. Chem. Soc.* **2006**, *128*, 14256–14257.

(20) Hagfeldt, A.; Grätzel, M. *Chem. Rev.* **1995**, *95*, 49–68.

(21) Ren, X.; Feng, Q.; Zhou, G.; Huang, C.-H.; Wang, Z.-S. *J. Phys. Chem. C* **2010**, *114*, 7190–7195.

(22) (a) Heimer, T. A.; D' Arcangelis, S. T.; Farzad, F.; Stipkala, J. M.; Meyer, G. J. *Inorg. Chem.* **1996**, *35*, 5319–5324. (b) Bonhote, P.; Cogniat, E.; Tingry, S.; Barbe, C.; Vlachopoulos, N.; Lenzmann, F.; Comte, P.; Grätzel, M. *J. Phys. Chem. B* **1998**, *102*, 1498–1507.

(23) Kopidakis, N.; Neale, N. R.; Frank, A. J. *J. Phys. Chem. B* **2006**, *110*, 12485–12489.